

Geophysical Research Letters[®]



RESEARCH LETTER

10.1029/2022GL102444

Controls on Ice Cliff Distribution and Characteristics on Debris-Covered Glaciers

Key Points:

- We derived an unprecedented data set of 37,537 ice cliffs and their characteristics across 86 debris-covered glaciers in High Mountain Asia
- We find that 38.9% of the cliffs are stream-influenced, 19.5% pond-influenced and 19.7% are crevasse-originated
- Ice cliff distribution can be predicted by velocity, as an indicator of the dynamics and state of evolution of debris-covered glaciers

Marin Kneib^{1,2} , Catriona L. Fyffe³ , Evan S. Miles¹ , Shayna Lindemann¹, Thomas E. Shaw¹, Pascal Buri¹ , Michael McCarthy¹ , Boris Ouvry⁴, Andreas Vieli⁴ , Yota Sato⁵, Philip D. A. Kraaijenbrink⁶ , Chuanxi Zhao^{7,8}, Peter Molnar² , and Francesca Pellicciotti^{1,3} 

¹High Mountain Glaciers and Hydrology Group, Swiss Federal Institute, WSL, Birmensdorf, Switzerland, ²Institute of Environmental Engineering, ETH Zürich, Zürich, Switzerland, ³Department of Geography and Environmental Sciences, Northumbria University, Newcastle Upon Tyne, UK, ⁴Department of Geography, University of Zurich, Zurich, Switzerland, ⁵Graduate School of Environmental Studies, Nagoya University, Nagoya, Japan, ⁶Department of Physical Geography, Utrecht University, Utrecht, The Netherlands, ⁷College of Earth and Environmental Sciences, Lanzhou University, Lanzhou, China, ⁸State Key Laboratory of Tibetan Plateau Earth System, Environment and Resources (TPESER), Institute of Tibetan Plateau Research, Chinese Academy of Sciences, Beijing, China

Supporting Information:

Supporting Information may be found in the online version of this article.

Correspondence to:

M. Kneib,
marin.kneib@gmail.com

Citation:

Kneib, M., Fyffe, C. L., Miles, E. S., Lindemann, S., Shaw, T. E., Buri, P., et al. (2023). Controls on ice cliff distribution and characteristics on debris-covered glaciers. *Geophysical Research Letters*, 50, e2022GL102444. <https://doi.org/10.1029/2022GL102444>

Received 6 DEC 2022

Accepted 7 MAR 2023

Author Contributions:

Conceptualization: Marin Kneib, Catriona L. Fyffe, Evan S. Miles, Thomas E. Shaw, Pascal Buri, Michael McCarthy, Yota Sato, Philip D. A. Kraaijenbrink, Peter Molnar, Francesca Pellicciotti

Data curation: Marin Kneib

Formal analysis: Marin Kneib, Evan S. Miles

Funding acquisition: Francesca Pellicciotti

Investigation: Marin Kneib, Shayna Lindemann

Methodology: Marin Kneib

Abstract Ice cliff distribution plays a major role in determining the melt of debris-covered glaciers but its controls are largely unknown. We assembled a data set of 37,537 ice cliffs and determined their characteristics across 86 debris-covered glaciers within High Mountain Asia (HMA). We find that 38.9% of the cliffs are stream-influenced, 19.5% pond-influenced and 19.7% are crevasse-originated. Surface velocity is the main predictor of cliff distribution at both local and glacier scale, indicating its dependence on the dynamic state and hence evolution stage of debris-covered glacier tongues. Supraglacial ponds contribute to maintaining cliffs in areas of thicker debris, but this is only possible if water accumulates at the surface. Overall, total cliff density decreases exponentially with debris thickness as soon as the debris layer reaches a thickness of over 10 cm.

Plain Language Summary Debris-covered glaciers are common throughout the world's mountain ranges and are characterized by the presence of steep ice cliffs among the debris-covered ice. It is well-known that the cliffs are responsible for a large portion of the melt of these glaciers but the controls on their formation, development and distribution across glaciers remains poorly understood. Novel mapping approaches combined with high-resolution satellite and drone products enabled us to disentangle some of these controls and to show that the ice cliffs are generally formed and maintained by the surface hydrology (ponds or streams) or by the opening of crevasses. As a result, they depend both at the local and glacier scale on the dynamic state of the glaciers as well as the evolution stage of their debris cover. This provides a pathway to better represent their contribution to glacier melt in predictive glacier models.

1. Introduction

Debris-covered glaciers are found in all mountain ranges (Scherler et al., 2018), and supraglacial debris extents and thickness are expected to increase in a warming climate (Compagno et al., 2022; Herreid & Pellicciotti, 2020; Stokes et al., 2007). However, despite considerable recent advances, modeling the mass balances of these glaciers remains challenging (Rounce et al., 2021). This is partly due to the presence of supraglacial ice cliffs, which melt up to 20 times faster than the surrounding debris-covered ice, therefore compensating for the relatively well constrained debris insulating effect (Anderson, Armstrong, Anderson, & Buri, 2021; Brun et al., 2018; E. S. Miles, Willis, et al., 2018; Reid & Brock, 2014; Sakai et al., 1998, 2002). In one catchment in High Mountain Asia (HMA) ice cliffs were shown to contribute $17\% \pm 4\%$ of the melt of the debris-covered ice (Buri et al., 2021). This has major implications for the mass balance of debris-covered glaciers (Pellicciotti et al., 2015) and their long-term evolution (Ferguson & Vieli, 2021; Racoviteanu et al., 2022).

While models accurately simulate the energy and mass balance contribution of individual ice cliffs (Buri et al., 2016; Kneib et al., 2022), their application at large spatial scales is limited by our understanding of the controls of ice cliff distribution. Indeed, estimates of ice cliff density are difficult to make (Anderson, Armstrong, Anderson, & Buri, 2021; Herreid & Pellicciotti, 2018; Kneib et al., 2020) and vary widely in time and space, between 1% and 15% of the debris-covered area (e.g., Falaschi et al., 2021; Kneib et al., 2021; Loriaux & Ruiz, 2021; Sato et al., 2021; Steiner et al., 2019; Watson, Quincey, Smith, et al., 2017). Remote sensing

© 2023. The Authors.

This is an open access article under the terms of the [Creative Commons Attribution License](https://creativecommons.org/licenses/by/4.0/), which permits use, distribution and reproduction in any medium, provided the original work is properly cited.

Project Administration: Francesca Pellicciotti
Resources: Thomas E. Shaw, Michael McCarthy, Boris Ouvry, Andreas Vieli, Yota Sato, Philip D. A. Kraaijenbrink, Chuanxi Zhao, Francesca Pellicciotti
Software: Evan S. Miles
Supervision: Peter Molnar, Francesca Pellicciotti
Validation: Marin Kneib
Visualization: Marin Kneib, Evan S. Miles
Writing – original draft: Marin Kneib
Writing – review & editing: Catriona L. Fyffe, Evan S. Miles, Thomas E. Shaw, Pascal Buri, Michael McCarthy, Boris Ouvry, Andreas Vieli, Francesca Pellicciotti

studies have shown that cliffs are often associated with ponds (Steiner et al., 2019; Watson, Quincey, Carrivick, & Smith, 2017), hinting at a preferential location of ice cliffs where lower glacier longitudinal gradient and surface velocities promote surface ponding (Bolch et al., 2008; Quincey & Glasser, 2009; Quincey et al., 2007; Racoviteanu et al., 2021; Reynolds, 2000; Sakai & Fujita, 2010; Salerno et al., 2012). Other observations indicate that ice cliffs preferentially develop at the confluence of glacial tributaries, in locations of high compressive strain rates, and areas of thinner debris (Anderson, Armstrong, Anderson, & Buri, 2021; Anderson, Armstrong, Anderson, Scherler, & Petersen, 2021; Benn et al., 2012; Kraaijenbrink et al., 2016; Steiner et al., 2019; Watson, Quincey, Carrivick, & Smith, 2017). However, the lack of consistent observations of cliff distribution makes it difficult to include ice cliffs in predictive glacier models in a way that accounts for their spatial distribution and temporal evolution.

Ice cliff survival is linked to debris stability, which is a function of local slope, debris thickness and water content, as well as undercutting by streams or ponds (Moore, 2018). The local slope can change in relatively short time scales with differential melt caused by heterogeneous debris thicknesses (Moore, 2021; Nicholson et al., 2018; Sharp, 1949), which results in the surface being particularly hummocky where the debris gets thicker than 20–30 cm (Bartlett et al., 2020; King et al., 2020). Slope undercutting and destabilization by streams or ponds has been observed to be one of the main triggers for ice cliff formation (Mölg et al., 2019; Röhl, 2006, 2008; Sakai & Takeuchi, 2000) and persistence (Benn et al., 2001, 2012; Brun et al., 2016; Kneib et al., 2022; Sato et al., 2021; Watson, Quincey, Smith, et al., 2017). Other hypothesized cliff formation mechanisms based on field and remote sensing observations include crevasse opening (Reid & Brock, 2014; Steiner et al., 2019) or the collapse of englacial conduits (Egli et al., 2021; Gulley et al., 2009; Immerzeel et al., 2014; E. S. Miles, Watson, et al., 2018; K. E. Miles et al., 2020; Sakai & Takeuchi, 2000), but these hypotheses have never been tested quantitatively.

In this study, we therefore (a) map ice cliffs across 86 glaciers in HMA, (b) determine their physical characteristics, (c) attribute their distribution to potential local and glacier-wide controlling factors.

2. Data and Methods

We derived a number of data sets to link ice cliff distribution with other surface features (streams, ponds, crevasses) and main glacier characteristics (debris-cover, dynamics, ruggedness). We used 14 Pléiades stereo-images acquired between 2017 and 2021 to derive 2 m-resolution multi-spectral images and Digital Elevation Models (DEMs) covering 86 debris-covered glaciers across HMA (Berthier et al., 2014; Shean et al., 2016; Figure 1; Table S2 in Supporting Information S1), 70 of which had more than 65% of their debris-covered area that could be classified after removal of clouds, shadows and fresh-snow (Table S3 in Supporting Information S1). The DEMs were used to derive surface slope and aspect, the local topographic ruggedness, which we defined as the percentage of area for which the Statistical Measure of Relief (SMR) calculated over a 8 m window (16 pixels) was greater than 50 m (King et al., 2020), as well as supraglacial channels (Schwanghart & Scherler, 2014; Text S2 in Supporting Information S1). The multi-spectral images were used to manually update the glacier and debris outlines of the RGI 6.0 (Pfeffer et al., 2014; Scherler et al., 2018). Glacier longitudinal gradient was computed using the 30 m resolution AW3D DEM (Dehecq et al., 2019; Tadono et al., 2014) and combined with glacier ice thicknesses (Farinotti et al., 2019) to estimate driving stress over a distance of two ice thicknesses. Distributed glacier velocity, compressive and tensile strain rates were obtained from the global 50 m resolution composite by Millan et al. (2022). We additionally used the distributed debris thickness data set of McCarthy et al. (2022) for all glaciers larger than 2 km² (64 glaciers, 47 of which have more than 65% of their debris-covered area that could be classified). All these data sets were aggregated (a) in 500 m distance bins along the glacier flowlines (Kienholz et al., 2014; King et al., 2020) and (b) for each glacier. Data gaps within the bins were filled using a nearest neighbor interpolation.

Ice cliffs and ponds were derived automatically in each Pléiades scene following the Spectral Curvature method for cliffs, which is based solely on spectral characteristics (Kneib et al., 2020), and the Normalized Difference Water Index (NDWI) for ponds (McFeeters, 1996; E. S. Miles et al., 2017; Watson et al., 2016, 2018; Text S2 in Supporting Information S1). Hence, in our study any exposed ice appearing amidst the debris, thus likely to undergo “enhanced” melt locally, is defined as an ice cliff. Some of these features were clearly identifiable as crevasse-originated due to their elongated, straight or slightly curved shapes and these zones were outlined manually. Past studies have only examined high-relief (several meters) ice cliffs, but here our interest is in all exposed

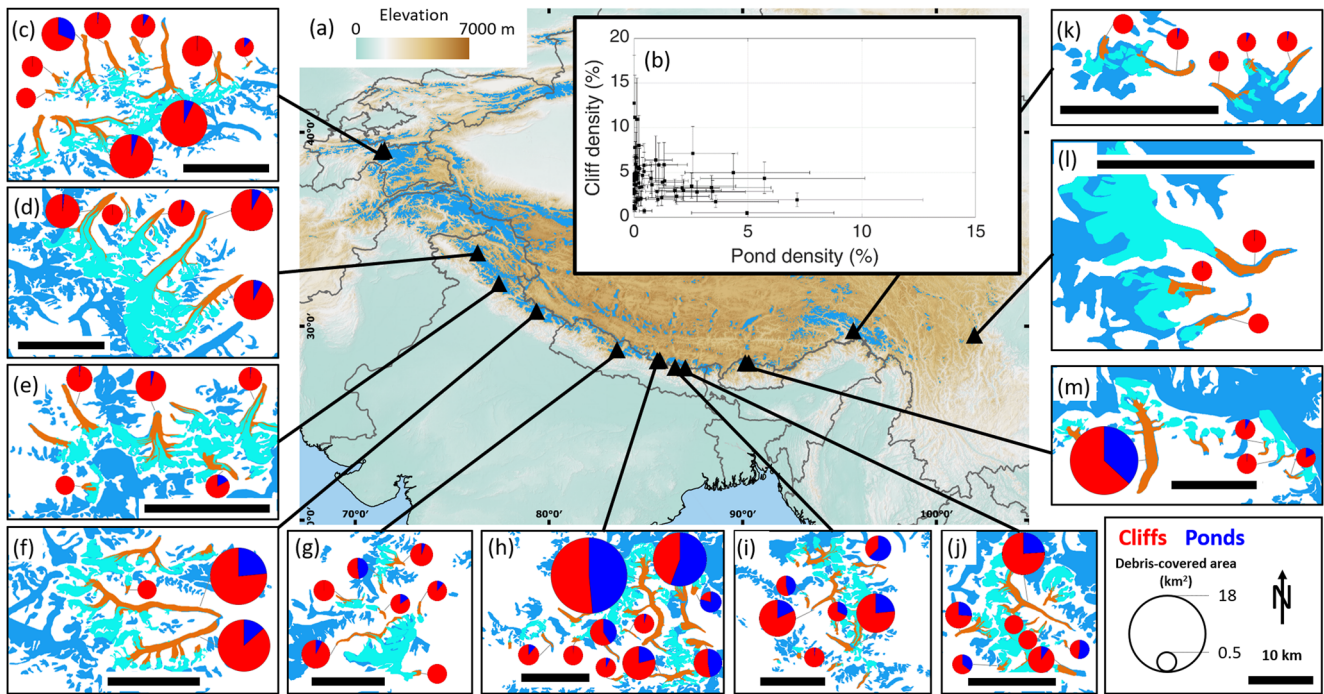


Figure 1. (a) Map of High Mountain Asia with each triangle representing one of the 14 Pléiades scenes (some scenes are very close to each other) and the boxes to the side (c–m) showing a zoomed view of the glaciers in these areas. The background is the GTOPO 30 arc s (~ 1 km) Digital Elevation Model, and the glacierised areas are indicated in blue. The inset boxes show the glacier RGI 6.0 outlines in dark blue, the glaciers visible in the Pléiades images in turquoise and their debris-covered areas in brown. The pie charts are scaled to the absolute size of the debris-covered areas and show the relative proportion of ponds (dark blue) and cliffs (red) for each glacier for which more than 65% of their debris-covered area could be classified. (b) Cliff and pond density of each of these glaciers. The bars show the uncertainties.

ice in the debris-covered area, so we include smaller features common for thin-debris areas, such as crevasses, which similarly enhance surface ablation (Colgan et al., 2016).

3. Results

3.1. Influence of Supraglacial Hydrology on Ice Cliff Distribution

Cliffs are preferentially located in the vicinity of ponds and streams, as their density strongly decreases with distance from these hydrological features (Figure 2a), and, averaged per glacier, a large majority (85%) of the ponds are within 40 m of at least one neighboring cliff (Figure 2b). The analysis of high-resolution (<0.2 m) multitemporal UAV orthoimages and DEMs at five of the glaciers in this study shows that 79% of the newly formed cliff area from 202 cliff formation events is related to the presence of streams or ponds, which indicates that these hydrological features directly influence ice cliff formation (Text S1 and Figure S2 in Supporting Information S1). Such association is further confirmed by field observations (Figure 2g–2i) at numerous sites for both the formation and persistence of ice cliffs (Anderson, Armstrong, Anderson, Scherler, & Petersen, 2021; Brun et al., 2016; Kneib et al., 2021; E. S. Miles et al., 2016; Mölg et al., 2020; Sato et al., 2021). This association between streams and cliffs or ponds and cliffs, and the decreasing density of cliffs with distance from these features (Figure 2a) leads us to define a 40 m-buffer around ponds and streams within which we classify the cliff pixels as pond-influenced or stream-influenced (Figure 2). With this definition, pond-influenced cliffs account for 19.5% and stream-influenced cliffs for 38.9% of the total cliff area (Figure 2c). In addition, crevasse-originated cliffs represent 19.7% of the cliff area across all glaciers. They are mostly located in the upper one-third of the debris-covered areas but also appear lower down glacier, at shear margins, and can be related to proglacial lakes or lateral streams entering the glacier (Figure S3 in Supporting Information S1). The remaining cliffs, which are not proximal to crevasses, ponds or streams, are qualified as undefined. The stream mapping parameters and choice of buffer size have little influence on this classification (Figure S9 in Supporting Information S1).

The slope and density of ice cliffs vary between categories, while this is less the case for aspect and size (Figure 2d–2f, Figure S10 in Supporting Information S1). Crevasse-originated cliffs are usually more densely

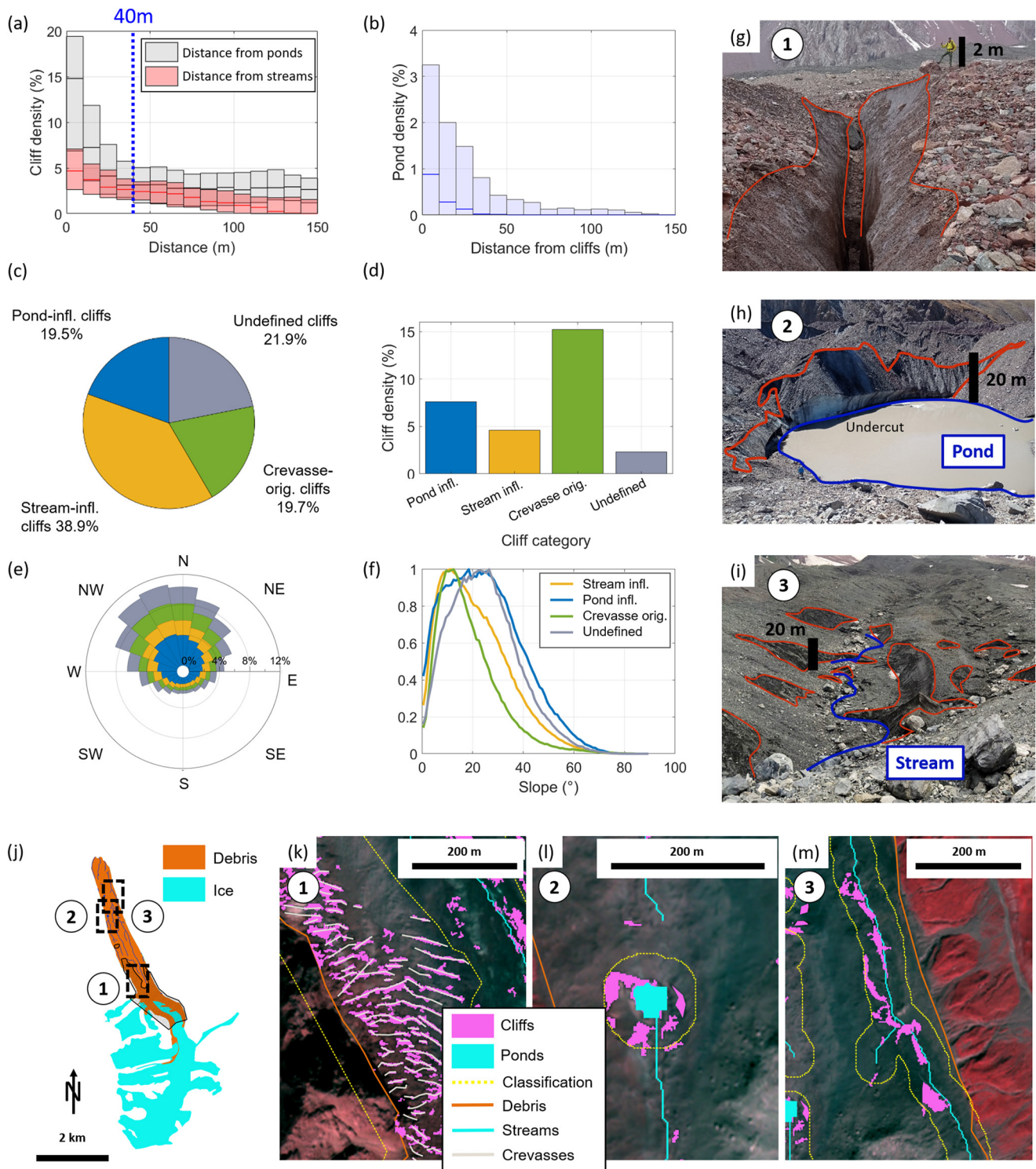


Figure 2. (a) Cliff density for all glaciers as a function of distance from ponds (gray) after removal of the crevassed-areas and from streams (red), after removal of the pond-influenced cliffs. The box plots indicate the median, 25th and 75th percentiles of the cliff density within each 10 m bin for each glacier. The blue dotted line shows the 40 m buffers. (b) Pond density for all glaciers as a function of distance from cliffs. (c) Area proportion of undefined, pond- and stream-influenced cliffs and crevasse-originated cliffs across all debris-covered glaciers. (d) Ice cliff density within buffer areas. (e) Aspect and (f) normalized slope distribution for all cliff pixels. (j) Example of classification of ice cliffs from Kyzylsu Glacier, Tajikistan: 1/crevassed-areas, 2/pond-influenced cliffs and 3/stream-influenced cliffs, with the pictures (g–i) and Pléiades view (k–m) of the corresponding zones. Image credit: M. Kneib and E. S. Miles. Background of (k–m) is the Pléiades false-color multispectral image (19 September 2021). Pléiades © CNES 2021, Distribution AIRBUS DS.

distributed (15.2% of crevassed zones), followed by the pond-influenced (6.7% of buffer area around ponds), stream-influenced (4.3% of buffer area around streams) and undefined cliffs (2.1% of remaining area). Despite a variety of glacier aspects (Table S3 in Supporting Information S1), there is a clear preferential cliff aspect distribution in the NNW direction for all categories.

3.2. Controls on Ice Cliff Distribution

The variables associated with ice cliff distribution vary depending on the category of cliff considered (Figure 3, Figure S11, and Table S5 in Supporting Information S1). Stream-influenced and undefined cliffs follow a similar distribution for all predictors (Figure S11 in Supporting Information S1), which could indicate that a majority of the undefined cliffs were formerly stream-influenced and backwasted away from the channels. 80% of stream-influenced cliffs are located in areas with debris estimated to be thinner than 33 cm, while 45% of the pond-influenced cliffs are located in areas with thicker debris (Figure S11 in Supporting Information S1).

This results in the total cliff density decreasing exponentially ($Y = 5.8e^{-\frac{x}{2}}, R^2 = 0.73$) when debris gets thicker than 10 cm (Figure 3a, Figure S12 in Supporting Information S1). Furthermore, crevasse-originated and pond-influenced cliffs have a clearly contrasting response to the different controls investigated. Indeed, 80% of the crevasse-originated cliffs are located in areas with surface velocities higher than 13 m yr^{-1} or in areas with debris thinner than 20 cm (Figure S11 in Supporting Information S1). Pond-influenced cliffs clearly depend on pond density, and are thus preferentially located in non-dynamic areas with lower longitudinal gradient and velocity and with thicker debris (Figure 3, Figures S11 and S13 in Supporting Information S1).

3.3. Ice Cliff Dependence on Glacier State

There is a clear relationship between mean surface velocity across the debris-covered area and cliff density (Figure 4, Figure S14 in Supporting Information S1) while the influence of climatic variables is limited (Figure S15 in Supporting Information S1). Cliff density decreases with decreasing velocity, up to a point where the trajectory seems to bifurcate. The debris-covered tongues with the highest cliff density and fastest velocity have a larger proportion of crevasse-originated cliffs (state 1, Figure 4). At slower velocities ($<10 \text{ m yr}^{-1}$), two trajectories are apparent: (a) glaciers with a large proportion ($>1/3$) of pond-influenced cliffs and higher cliff densities (state 3a, Figure 4), and (b) glaciers with a majority of stream-influenced cliffs, which tend to have lower cliff densities (state 3b, Figure 4). The majority of the glaciers are found at an intermediary stage between these three end-members, with a decreasing proportion of crevasse-originated cliffs and an increasing proportion of stream- and pond-influenced cliffs as velocity decreases (state 2, Figure 4).

4. Discussion and Conclusions

We have identified the presence of supraglacial streams and ponds, along with the opening of crevasses, to be the main mechanisms responsible for ice cliff development, and observed that cliffs get reburied when they backwaste away from these supraglacial features (Figure 2a).

4.1. Ice Cliff Distribution and Glacier State

Velocity stands out as a main correlate of ice cliff density both at the local and glacier scale (Figures 3 and 4). Interlinkages of glacier velocity with other variables means that the cliff density also responds to other local controls, and debris thickness especially, although each category of cliffs responds differently (Figure 3). The distribution of ice cliffs therefore depends on the glacier dynamics and state. A dynamic debris-covered glacier (mean surface velocity $>10 \text{ m yr}^{-1}$, Figures 4 and 5a, Figure S16a in Supporting Information S1) is usually characterized by thin debris and crevasses which comprise the majority of exposed ice and drain supraglacial streams. Glacier slow-down results in reduced strain rates and the limitation of crevasses to the upper sections of the debris-covered area and their eventual disappearance (Figure 3j, Figure S16b in Supporting Information S1), the extension of stream-influenced cliffs through debris destabilization and thermo-erosional undercutting (Moore, 2018; Figure 3a) and possibly the emergence of pond-influenced cliffs. Ponds maintain cliffs in more stagnant zones of thicker debris, also characterized by low longitudinal gradients and driving stress as well as increased hummock prevalence (Benn et al., 2017; Steiner et al., 2019; Watson, Quincey, Carrivick, & Smith, 2017; Figure 5c). Such evolution has been observed on other glaciers: on Zmutt Glacier, where it was linked to the development of supraglacial valleys driven by stream

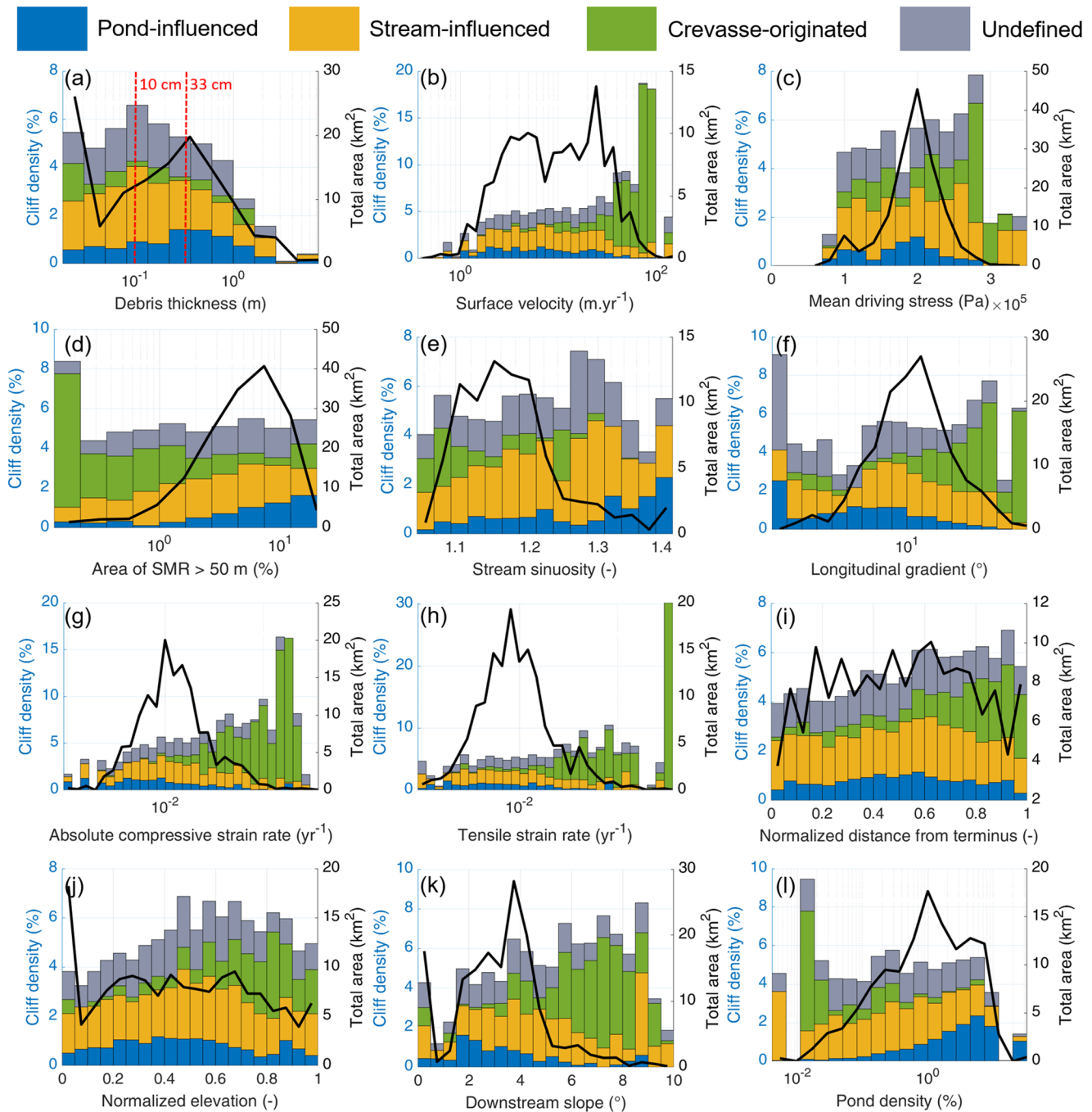


Figure 3. Mean cliff density split by cliff category for all bins of all glaciers where more than 65% of the debris-covered area could be classified as a function of (a) debris thickness, (b) surface velocity, (c) mean driving stress, (d) ruggedness, (e) stream sinuosity, (f) longitudinal gradient, (g) absolute compressive strain rate, (h) tensile strain rate, (i) normalized distance from terminus, (j) normalized elevation above terminus, (k) downstream slope to terminus, and (l) pond density. The black line shows the area distribution of all the bins.

incision (Mölg et al., 2020); and on Khumbu Glacier, where high relief zones characterized by growing cliffs and ponds have developed as the glacier has slowed (King et al., 2020; Rowan et al., 2021). Our large data set enables us to show that this evolution holds across a large number of glaciers, and to identify predictors of cliff type and distribution. The development of large pond-influenced cliffs however requires the accumulation of water in surface depressions, which occurs for larger glaciers with lower longitudinal gradients (Figures 4 and 5c, Figure S13 in Supporting Information S1). Most HMA glaciers in this stage of evolution are located in the Central and Eastern Himalaya (Benn et al., 2012, 2017; Racoviteanu et al., 2021; Watson et al., 2016; Watson, Quincey, Carrivick, &

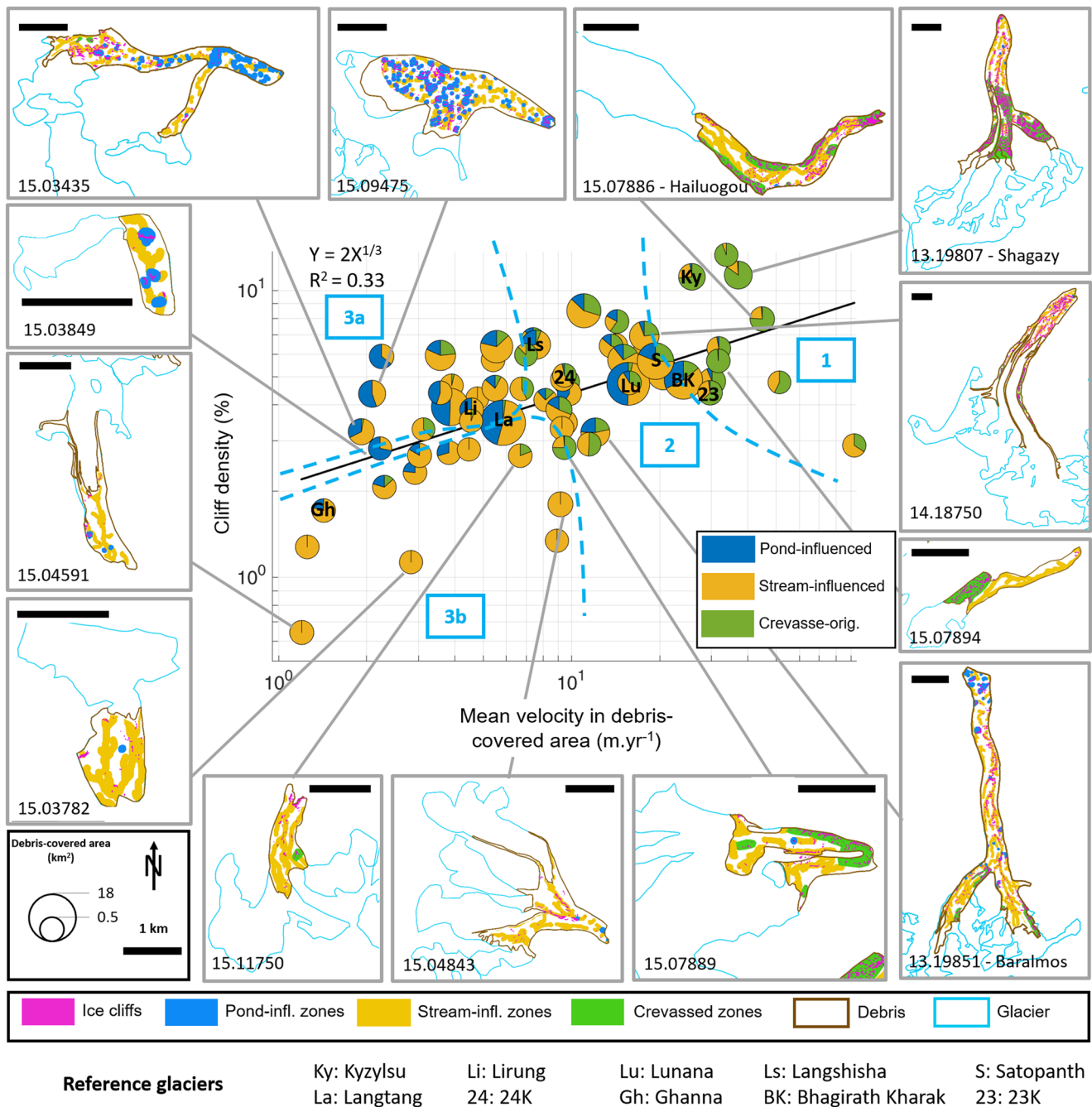


Figure 4. Glacier-wide cliff density as a function of mean velocity in the debris-covered area for all glaciers where more than 65% of the debris-covered area could be classified. The proportion of undefined cliffs was not represented for readability. The boxes show example glaciers with their surface classifications. Some reference glaciers are indicated in the main plot in black. The expression and R^2 of the black linear regression are indicated in the upper left corner. In light blue are shown four glacier clusters.

Smith, 2017; Figure 1). However, some glaciers do not develop such drainage systems due to their relative steepness and small size, resulting in lower ice cliff densities (Figures 4 and 5d, Figure S16d in Supporting Information S1).

4.2. Implications for Glacier Mass Balance

We have shown that ice cliff density and characteristics depend on the evolution state of the debris-covered glacier (Figure 5), which is controlled mainly by dynamics (velocity) and debris thickness. Leveraging this new

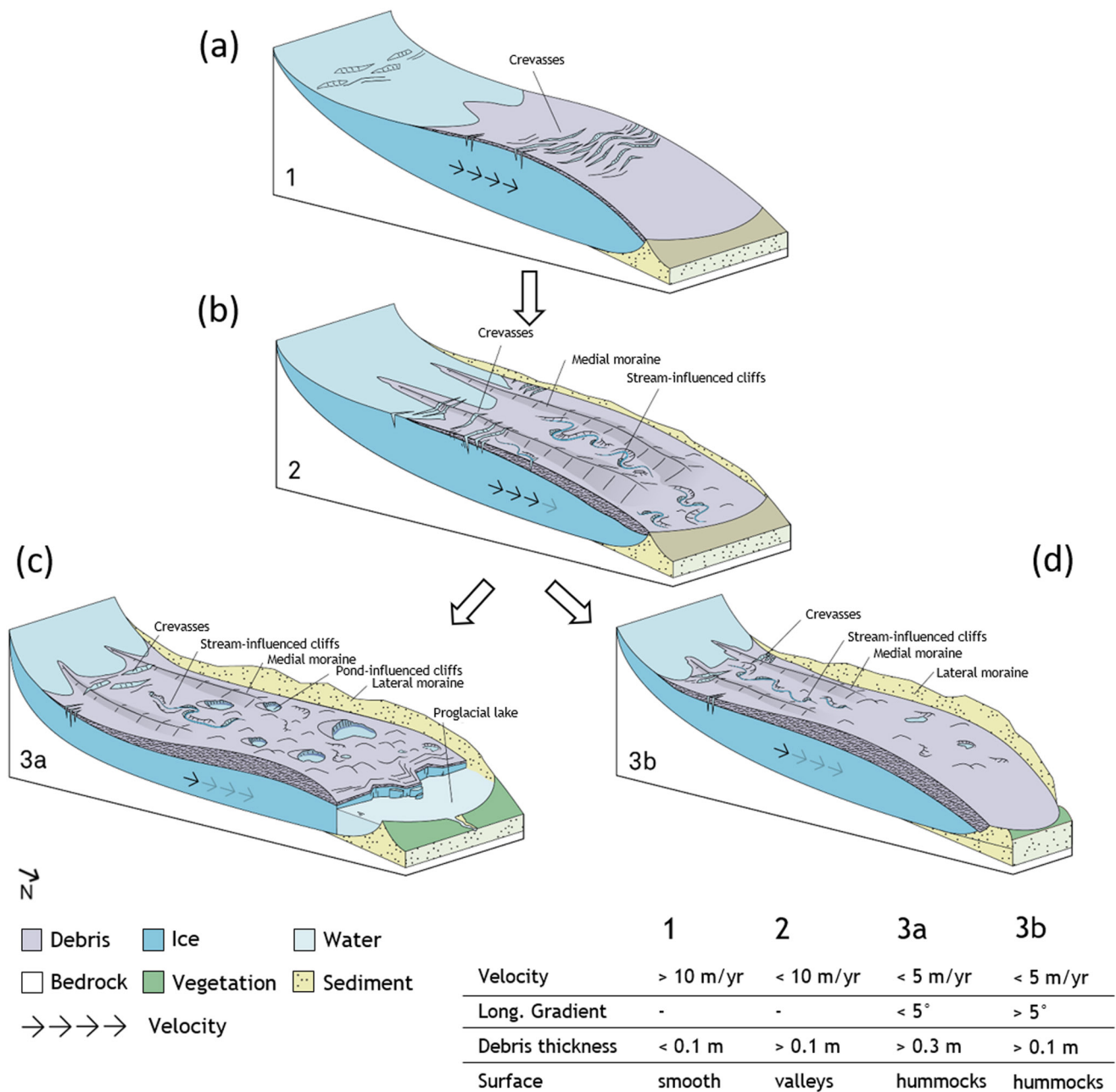


Figure 5. The four glacier evolution states, with their ice cliff distributions. State 1: fast flowing glacier with thin debris and extensive crevassing. State 2: advanced debris cover, with thicker debris and lower velocities enabling the development of supraglacial valleys and stream-influenced cliffs in the non-crevassed areas. State 3a: large stagnating debris-covered tongues, characterized by hummocks, thick debris and ponds maintaining cliffs in these zones. State 3b: stagnating tongues with thick debris, but high enough longitudinal gradient or low enough surface meltwater to prevent the formation of ponds and therefore the survival of cliffs. Figure credit: Martin Heynen.

understanding of how glacier stage affects the presence of cliffs on their surfaces, we have provided the distribution of each type of cliff on glaciers at different stages of evolution (Figures 3 and 4, Figure S16 and Table S5 in Supporting Information S1). Future efforts should focus on testing this framework by substantially expanding the number of data points, including glaciers at distinct stages, as well as glaciers in other mountain regions, with different topo-climatic characteristics. Most of the debris-covered glaciers that have been the object of detailed investigations belong to glacier states 2 and 3 and efforts should be made to explore the whole range of evolution when targeting field studies. Already at this stage, however, the relationships detailed in this study outline a framework to estimate ice cliff distribution based on glacier flow characteristics, which are usually available

in prognostic flow models, and debris thickness, without having to map the cliffs. Combined with cliff melt enhancement factors (E. S. Miles et al., 2022), this would allow long term estimation of the contribution of ice cliffs to debris-covered glacier mass balance—representing a key modeling advance.

Future work should also target the contribution of crevasse-originated cliffs to glacier mass balance. Indeed, these features would likely enhance melt even more than traditional stream- and pond-influenced cliffs due to greater surface roughness at their location increasing turbulent fluxes, and additional reflected shortwave contributions from the opposite crevasse walls (Cathles et al., 2011; Colgan et al., 2016; Pfeffer & Bretherton, 1987; Purdie et al., 2022). Time-lapse images actually show the upper walls of crevasses backwasting as traditional ice cliffs would (Figure S17 in Supporting Information S1). Furthermore, their longer-term evolution and influence on shaping the debris-covered glacier surface remains unclear (Kirkbride & Deline, 2013).

Data Availability Statement

The glacier, debris, crevasse, cliff and pond outlines are available on Zenodo (<https://doi.org/10.5281/zenodo.7602582>). Other data sets used include surface velocity from Millan et al. (2022), climate data from ERA5-Land (Muñoz Sabater, 2019), RGI 6.0. glacier outlines (<https://nsidc.org/data/nsidc-0770/versions/6>), the AW3D 30m DEM (Tadono et al., 2014) and ice thicknesses (Farinotti et al., 2019). Atmospherically-corrected Sentinel-2 images prior to 2019 were obtained from CNES through the PEPS platform (Hagolle et al., 2015). From 2019 and later they were processed directly in Google Earth Engine.

References

- Anderson, L. S., Armstrong, W. H., Anderson, R. S., & Buri, P. (2021). Debris cover and the thinning of Kennicott Glacier, Alaska: In situ measurements, automated ice cliff delineation and distributed melt estimates. *The Cryosphere*, 15(1), 265–282. <https://doi.org/10.5194/tc-15-265-2021>
- Anderson, L. S., Armstrong, W. H., Anderson, R. S., Scherler, D., & Petersen, E. (2021). The causes of debris-covered glacier thinning: Evidence for the importance of ice dynamics from Kennicott glacier, Alaska. *Frontiers of Earth Science*, 9, 723. <https://doi.org/10.3389/FEART.2021.680995>
- Bartlett, O. T., Ng, F. S. L., & Rowan, A. V. (2020). Morphology and evolution of supraglacial hummocks on debris-covered Himalayan glaciers. *Earth Surface Processes and Landforms*, 46(3), 525–539. <https://doi.org/10.1002/esp.5043>
- Benn, D. I., Bolch, T., Hands, K., Gulle, J., Luckman, A., Nicholson, L. I., et al. (2012). Response of debris-covered glaciers in the Mount Everest region to recent warming, and implications for outburst flood hazards. *Earth-Science Reviews*, 114(1–2), 156–174. <https://doi.org/10.1016/j.earscirev.2012.03.008>
- Benn, D. I., Thompson, S., Gulle, J., Mertes, J., Luckman, A., & Nicholson, L. (2017). Structure and evolution of the drainage system of a Himalayan debris-covered glacier, and its relationship with patterns of mass loss. *The Cryosphere*, 11(5), 2247–2264. <https://doi.org/10.5194/tc-11-2247-2017>
- Benn, D. I., Wiseman, S., & Hands, K. A. (2001). Growth and drainage of supraglacial lakes on debris-mantled Ngozumpa Glacier, Khumbu Himal, Nepal. *Journal of Glaciology*, 47(159), 626–638. <https://doi.org/10.3189/172756501781831729>
- Berthier, E., Vincent, C., Magnússon, E., Gunnlaugsson, Á. P., Pitte, P., Le Meur, E., et al. (2014). Glacier topography and elevation changes derived from Pléiades sub-meter stereo images. *The Cryosphere*, 8(6), 2275–2291. <https://doi.org/10.5194/tc-8-2275-2014>
- Bolch, T., Buchroithner, M. F., Peters, J., Baessler, M., & Bajracharya, S. (2008). Identification of glacier motion and potentially dangerous glacial lakes in the Mt. Everest region/Nepal using spaceborne imagery. *Natural Hazards and Earth System Sciences*, 8(6), 1329–1340. <https://doi.org/10.5194/nhess-8-1329-2008>
- Brun, F., Buri, P., Miles, E. S., Wagnon, P., Steiner, J., Berthier, E., et al. (2016). Quantifying volume loss from ice cliffs on debris-covered glaciers using high-resolution terrestrial and aerial photogrammetry. *Journal of Glaciology*, 62(234), 684–695. <https://doi.org/10.1017/jog.2016.54>
- Brun, F., Wagnon, P., Berthier, E., Shea, J. M., Immerzeel, W. W., Kraaijenbrink, P. D. A., et al. (2018). Ice cliff contribution to the tongue-wide ablation of Changri Nup Glacier, Nepal, central Himalaya. *The Cryosphere*, 12(11), 3439–3457. <https://doi.org/10.5194/tc-12-3439-2018>
- Buri, P., Miles, E. S., Steiner, J. F., Ragettli, S., & Pellicciotti, F. (2021). Supraglacial ice cliffs can substantially increase the mass loss of debris-covered glaciers. *Geophysical Research Letters*, 48(6), e2020GL092150. <https://doi.org/10.1029/2020GL092150>
- Buri, P., Pellicciotti, F., Steiner, J. F., Miles, E. S., & Immerzeel, W. W. (2016). A grid-based model of backwasting of supraglacial ice cliffs on debris-covered glaciers. *Annals of Glaciology*, 57(71), 199–211. <https://doi.org/10.3189/2016AoG71A059>
- Cathles, L. M., Abbot, D. S., Bassis, J. N., & MacAyeal, D. R. (2011). Modeling surface-roughness/solar-ablation feedback: Application to small-scale surface channels and crevasses of the Greenland ice sheet. *Annals of Glaciology*, 52(59), 99–108. <https://doi.org/10.3189/172756411799096268>
- Colgan, W., Rajaram, H., Abdalati, W., McCutchan, C., Mottram, R., Moussavi, M. S., & Grigsby, S. (2016). Glacier crevasses: Observations, models, and mass balance implications. In *Reviews of geophysics*. Blackwell Publishing Ltd. <https://doi.org/10.1002/2015RG000504>
- Compagno, L., Huss, M., Miles, E. S., McCarthy, M. J., Zekollari, H., Dehecq, A., et al. (2022). Modelling supraglacial debris-cover evolution from the single-glacier to the regional scale: An application to High Mountain Asia. *The Cryosphere*, 16(5), 1697–1718. <https://doi.org/10.5194/tc-16-1697-2022>
- Dehecq, A., Gourmelen, N., Gardner, A. S., Brun, F., Goldberg, D., Nienow, P. W., et al. (2019). Twenty-first century glacier slowdown driven by mass loss in High Mountain Asia. *Nature Geoscience*, 12(1), 22–27. <https://doi.org/10.1038/s41561-018-0271-9>
- Egli, P. E., Belotti, B., Ouvry, B., Irving, J., & Lane, S. N. (2021). Subglacial channels, climate warming, and increasing frequency of alpine glacier snout collapse. *Geophysical Research Letters*, 48(21), e2021GL096031. <https://doi.org/10.1029/2021GL096031>
- Falaschi, D., Rivera, A., Lo Vecchio Repetto, A., Moragues, S., Villalba, R., Rastner, P., et al. (2021). Evolution of surface characteristics of three debris-covered glaciers in the Patagonian Andes from 1958 to 2020. *Frontiers of Earth Science*, 9, 447. <https://doi.org/10.3389/feart.2021.671854>

Acknowledgments

This project has received funding from the European Research Council (ERC) under the European Union's Horizon 2020 programme (grant agreement 772751) and from the Royal Society via a Newton Advanced Fellowship award (NA170325). The majority of the Pléiades stereo-pairs were provided by Etienne Berthier via the Pléiades Glacier Observatory (PGO) initiative of the French Space Agency (CNES). The remaining images were acquired through the CNES ISIS Programme. We thank the team of the Centre for Research on Glaciers at the Academy of Sciences of Tajikistan who enabled our 2021 fieldwork on Kyzylsu Glacier.

- Farinotti, D., Huss, M., Fürst, J. J., Landmann, J., Machguth, H., Maussion, F., & Pandit, A. (2019). A consensus estimate for the ice thickness distribution of all glaciers on Earth. *Nature Geoscience*, *12*(3), 168–173. <https://doi.org/10.1038/s41561-019-0300-3>
- Ferguson, J. C., & Vieli, A. (2021). Modelling steady states and the transient response of debris-covered glaciers. *The Cryosphere*, *15*(7), 3377–3399. <https://doi.org/10.5194/tc-15-3377-2021>
- Gulley, J. D., Benn, D. I., Scream, E., & Martin, J. (2009). Mechanisms of englacial conduit formation and their implications for subglacial recharge. *Quaternary Science Reviews*, *28*(19–20), 1984–1999. <https://doi.org/10.1016/j.quascirev.2009.04.002>
- Hagolle, O., Huc, M., Villa Pascual, D., & Dedieu, G. (2015). A multi-temporal and multi-spectral method to estimate aerosol optical thickness over land, for the atmospheric correction of FormoSat-2, LandSat, VENUS and Sentinel-2 images. *Remote Sensing*, *7*(3), 2668–2691. <https://doi.org/10.3390/rs70302668>
- Herreid, S., & Pellicciotti, F. (2018). Automated detection of ice cliffs within supraglacial debris cover. *The Cryosphere*, *12*(5), 1811–1829. <https://doi.org/10.5194/tc-12-1811-2018>
- Herreid, S., & Pellicciotti, F. (2020). The state of rock debris covering Earth's glaciers. *Nature Geoscience*, *13*(9), 1–7. <https://doi.org/10.1038/s41561-020-0615-0>
- Immerzeel, W. W., Kraaijenbrink, P. D. A., Shea, J. M., Shrestha, A. B., Pellicciotti, F., Bierkens, M. F. P., & De Jong, S. M. (2014). High-resolution monitoring of Himalayan glacier dynamics using unmanned aerial vehicles. *Remote Sensing of Environment*, *150*, 93–103. <https://doi.org/10.1016/j.rse.2014.04.025>
- Kienholz, C., Rich, J. L., Arendt, A. A., & Hock, R. (2014). A new method for deriving glacier centerlines applied to glaciers in Alaska and northwest Canada. *The Cryosphere*, *8*(2), 503–519. <https://doi.org/10.5194/tc-8-503-2014>
- King, O., Turner, A. G. D., Quincey, D. J., & Carrivick, J. L. (2020). Morphometric evolution of Everest region debris-covered glaciers. *Geomorphology*, *371*, 107422. <https://doi.org/10.1016/j.geomorph.2020.107422>
- Kirkbride, M. P., & Deline, P. (2013). The formation of supraglacial debris covers by primary dispersal from transverse englacial debris bands. *Earth Surface Processes and Landforms*, *38*(15), 1779–1792. <https://doi.org/10.1002/esp.3416>
- Kneib, M., Miles, E. S., Buri, P., Fugger, S., McCarthy, M., Shaw, T. E., et al. (2022). Sub-seasonal variability of supraglacial ice cliff melt rates and associated processes from time-lapse photogrammetry. *The Cryosphere*, *16*(11), 4701–4725. <https://doi.org/10.5194/tc-16-4701-2022>
- Kneib, M., Miles, E. S., Buri, P., Molnar, P., McCarthy, M., Fugger, S., & Pellicciotti, F. (2021). Interannual dynamics of ice cliff populations on debris-covered glaciers from remote sensing observations and stochastic modeling. *Journal of Geophysical Research: Earth Surface*, *126*(10), e2021JF006179. <https://doi.org/10.1029/2021JF006179>
- Kneib, M., Miles, E. S., Jola, S., Buri, P., Herreid, S., Bhattacharya, A., et al. (2020). Mapping ice cliffs on debris-covered glaciers using multispectral satellite images. *Remote Sensing of Environment*, *253*, 112201. <https://doi.org/10.1016/j.rse.2020.112201>
- Kraaijenbrink, P. D. A., Shea, J. M., Pellicciotti, F., De Jong, S. M., & Immerzeel, W. W. (2016). Object-based analysis of unmanned aerial vehicle imagery to map and characterise surface features on a debris-covered glacier. *Remote Sensing of Environment*, *186*, 581–595. <https://doi.org/10.1016/j.rse.2016.09.013>
- Loriaux, T., & Ruiz, L. (2021). Spatio-temporal distribution of supra-glacial ponds and ice cliffs on Verde glacier, Chile. *Frontiers of Earth Science*, *9*, 681071. <https://doi.org/10.3389/feart.2021.681071>
- McCarthy, M., Miles, E., Kneib, M., Buri, P., Fugger, S., & Pellicciotti, F. (2022). Supraglacial debris thickness and supply rate in High-Mountain Asia. *Communications Earth & Environment*, *3*(1), 269. <https://doi.org/10.1038/s43247-022-00588-2>
- McFeeters, S. K. (1996). The use of the Normalized Difference Water Index (NDWI) in the delineation of open water features. *International Journal of Remote Sensing*, *17*(7), 1425–1432. <https://doi.org/10.1080/01431169608948714>
- Miles, E., Pellicciotti, F., Willis, I., Steiner, J., Buri, P., & Arnold, N. (2016). Refined energy-balance modelling of a supraglacial pond, Langtang Khola, Nepal. *Annals of Glaciology*, *57*(71), 29–40. <https://doi.org/10.3189/2016AoG71A421>
- Miles, E. S., Steiner, J. F., Buri, P., Immerzeel, W. W., & Pellicciotti, F. (2022). Controls on the relative melt rates of debris-covered glacier surfaces. *Environmental Research Letters*, *17*(6), 064004. <https://doi.org/10.1088/1748-9326/ac6966>
- Miles, E. S., Watson, C. S., Brun, F., Berthier, E., Esteves, M., Quincey, D. J., et al. (2018). Glacial and geomorphic effects of a supraglacial lake drainage and outburst event, Everest region, Nepal Himalaya. *The Cryosphere*, *12*, 3891–3905. <https://doi.org/10.5194/tc-12-3891-2018>
- Miles, E. S., Willis, I., Buri, P., Steiner, J. F., Arnold, N. S., & Pellicciotti, F. (2018). Surface pond energy absorption across four Himalayan glaciers accounts for 1/8 of total catchment ice loss. *Geophysical Research Letters*, *45*(19), 10464–10473. <https://doi.org/10.1029/2018GL079678>
- Miles, E. S., Willis, I. C., Arnold, N. S., Steiner, J., & Pellicciotti, F. (2017). Spatial, seasonal and interannual variability of supraglacial ponds in the Langtang Valley of Nepal, 1999–2013. <https://doi.org/10.1017/jog.2016.120>
- Miles, K. E., Hubbard, B., Irvine-Fynn, T. D. L., Miles, E., Quincey, D. J., & Rowan, A. V. (2020). Hydrology of debris-covered glaciers in High Mountain Asia. *Earth-Science Reviews*, *207*, 103212. <https://doi.org/10.1016/j.earscirev.2020.103212>
- Millan, R., Mouginot, J., Rabatel, A., & Morlighem, M. (2022). Ice velocity and thickness of the world's glaciers. *Nature Geoscience*, *15*(2), 124–129. <https://doi.org/10.1038/s41561-021-00885-z>
- Mölg, N., Bolch, T., Walter, A., & Vieli, A. (2019). Unravelling the evolution of Zmuttgletscher and its debris cover since the end of the Little Ice Age. *The Cryosphere*, *13*(7), 1889–1909. <https://doi.org/10.5194/tc-13-1889-2019>
- Mölg, N., Ferguson, J., Bolch, T., & Vieli, A. (2020). On the influence of debris cover on glacier morphology: How high-relief structures evolve from smooth surfaces. *Geomorphology*, *357*, 107092. <https://doi.org/10.1016/j.geomorph.2020.107092>
- Moore, P. L. (2018). Stability of supraglacial debris. *Earth Surface Processes and Landforms*, *43*(1), 285–297. <https://doi.org/10.1002/esp.4244>
- Moore, P. L. (2021). Numerical simulation of supraglacial debris mobility: Implications for ablation and landform genesis. *Frontiers of Earth Science*, *9*, 710131. <https://doi.org/10.3389/feart.2021.710131>
- Muñoz Sabater, J. (2019). ERA5-land monthly averaged data from 1981 to present. In *Copernicus Climate Change Service (C3S) Climate Data Store (CDS)*. <https://doi.org/10.24381/cds.68d2bb30>
- Nicholson, L. I., McCarthy, M., Pritchard, H. D., & Willis, I. (2018). Supraglacial debris thickness variability: Impact on ablation and relation to terrain properties. *The Cryosphere*, *12*(12), 3719–3734. <https://doi.org/10.5194/tc-12-3719-2018>
- Pellicciotti, F., Stephan, C., Miles, E. S., Herreid, S., Immerzeel, W. W., & Bolch, T. (2015). Mass-balance changes of the debris-covered glaciers in the Langtang Himal, Nepal, from 1974 to 1999. *Journal of Glaciology*, *61*(226), 373–386. <https://doi.org/10.3189/2015JG13J237>
- Pfeffer, W. T., Arendt, A. A., Bliss, A., Bolch, T., Cogley, J. G., Gardner, A. S., et al. (2014). The Randolph Glacier Inventory: A globally complete inventory of glaciers. *Journal of Glaciology*, *60*(221), 537–552. <https://doi.org/10.3189/2014JG13J176>
- Pfeffer, W. T., & Bretherton, C. S. (1987). The effect of crevasses on the solar heating of a glacier surface. *The Physical Basis of Ice Sheet Modelling*, *170*, 191–205.
- Purdie, H., Zawar-Reza, P., Katurji, M., Schumacher, B., Kerr, T., & Bealing, P. (2022). Variability in the vertical temperature profile within crevasses at an alpine glacier. *Journal of Glaciology*, *69*(274), 1–15. <https://doi.org/10.1017/jog.2022.73>

- Quincey, D. J., & Glasser, N. F. (2009). Morphological and ice-dynamical changes on the Tasman Glacier, New Zealand, 1990–2007. *Global and Planetary Change*, 68(3), 185–197. <https://doi.org/10.1016/j.gloplacha.2009.05.003>
- Quincey, D. J., Richardson, S. D., Luckman, A., Lucas, R. M., Reynolds, J. M., Hambrey, M. J., & Glasser, N. F. (2007). Early recognition of glacial lake hazards in the Himalaya using remote sensing datasets. *Global and Planetary Change*, 56(1–2), 137–152. <https://doi.org/10.1016/j.gloplacha.2006.07.013>
- Racoviteanu, A. E., Glasser, N. F., Robson, B. A., Harrison, S., Millan, R., Kayastha, R. B., & Kayastha, R. (2022). Recent evolution of glaciers in the Manaslu region of Nepal from satellite imagery and UAV data (1970–2019). *Frontiers of Earth Science*, 9, 1200. <https://doi.org/10.3389/feart.2021.767317>
- Racoviteanu, A. E., Nicholson, L., & Glasser, N. F. (2021). Surface composition of debris-covered glaciers across the Himalaya using linear spectral unmixing of Landsat 8 OLI imagery. *The Cryosphere*, 15(9), 4557–4588. <https://doi.org/10.5194/tc-15-4557-2021>
- Reid, T. D., & Brock, B. W. (2014). Assessing ice-cliff backwasting and its contribution to total ablation of debris-covered Miage glacier, Mont Blanc massif, Italy. *Journal of Glaciology*, 60(219), 3–13. <https://doi.org/10.3189/2014JoG13J045>
- Reynolds, J. (2000). *On the formation of supraglacial lakes on debris-covered glaciers* (Vol. 264, pp. 153–161). IAHS-AISH Publication.
- Röhl, K. (2006). Thermo-erosional notch development at fresh-water-calving Tasman Glacier, New Zealand. *Journal of Glaciology*, 52(177), 203–213. <https://doi.org/10.3189/172756506781828773>
- Röhl, K. (2008). Characteristics and evolution of supraglacial ponds on debris-covered Tasman Glacier, New Zealand. *Journal of Glaciology*, 54(188), 867–880. <https://doi.org/10.3189/00221430878779861>
- Rounce, D. R., Hock, R., McNabb, R. W., Millan, R., Sommer, C., Braun, M. H., et al. (2021). Distributed global debris thickness estimates reveal debris significantly impacts glacier mass balance. *Geophysical Research Letters*, 48(8), e2020GL091311. <https://doi.org/10.1029/2020GL091311>
- Rowan, A. V., Egholm, D. L., Quincey, D. J., Hubbard, B., King, O., Miles, E. S., et al. (2021). The role of differential ablation and dynamic detachment in driving accelerating mass loss from a debris-covered Himalayan glacier. *Journal of Geophysical Research: Earth Surface*, 126(9), e2020JF005761. <https://doi.org/10.1029/2020JF005761>
- Sakai, A., & Fujita, K. (2010). Formation conditions of supraglacial lakes on debris covered glaciers in the Himalaya. *Journal of Glaciology*, 56(195), 177–181. <https://doi.org/10.3189/002214310791190785>
- Sakai, A., Nakawo, M., & Fujita, K. (1998). Melt rate of ice cliffs on the Lirung Glacier, Nepal Himalayas, 1996. *Bulletin of Glacier Research*, 16, 57–66.
- Sakai, A., Nakawo, M., & Fujita, K. (2002). Distribution characteristics and energy balance of ice cliffs on debris-covered glaciers, Nepal Himalaya. *Arctic Antarctic and Alpine Research*, 34(1), 12–19. <https://doi.org/10.1080/15230430.2002.12003463>
- Sakai, A., & Takeuchi, N. (2000). *Debris-covered glaciers*. IAHS Publications.
- Salerno, F., Thakuri, S., D'Agata, C., Smiraglia, C., Manfredi, E. C., Viviano, G., & Tartari, G. (2012). Glacial lake distribution in the Mount Everest region: Uncertainty of measurement and conditions of formation. *Global and Planetary Change*, 92–93, 30–39. <https://doi.org/10.1016/j.gloplacha.2012.04.001>
- Sato, Y., Fujita, K., Inoue, H., Sunako, S., Sakai, A., Tsushima, A., et al. (2021). Ice cliff dynamics of debris-covered Trakarding glacier in the Rolwaling region, Nepal Himalaya. *Frontiers of Earth Science*, 9, 398. <https://doi.org/10.3389/FEART.2021.623623/BIBTEX>
- Scherler, D., Wulf, H., & Gorelick, N. (2018). Global Assessment of supraglacial debris-cover extents. *Geophysical Research Letters*, 45(21), 11798–11805. <https://doi.org/10.1029/2018GL080158>
- Schwanghart, W., & Scherler, D. (2014). Short communication: TopoToolbox 2—MATLAB-based software for topographic analysis and modeling in Earth surface sciences. *Earth Surface Dynamics*, 2(1), 1–7. <https://doi.org/10.5194/esurf-2-1-2014>
- Sharp, R. P. (1949). Studies of superglacial debris on valley glaciers. *American Journal of Science*, 247(5), 289–315. <https://doi.org/10.2475/ajs.247.5.289>
- Shean, D. E., Alexandrov, O., Moratto, Z. M., Smith, B. E., Joughin, I. R., Porter, C., & Morin, P. (2016). An automated, open-source pipeline for mass production of digital elevation models (DEMs) from very-high-resolution commercial stereo satellite imagery. *ISPRS Journal of Photogrammetry and Remote Sensing*, 116, 101–117. <https://doi.org/10.1016/j.isprsjprs.2016.03.012>
- Steiner, J. F., Buri, P., Miles, E. S., Ragettli, S., & Pellicciotti, F. (2019). Supraglacial ice cliffs and ponds on debris-covered glaciers: Spatio-temporal distribution and characteristics. *Journal of Glaciology*, 65(252), 617–632. <https://doi.org/10.1017/jog.2019.40>
- Stokes, C. R., Popovnin, V., Aleynikov, A., Gurney, S. D., & Shahgedanova, M. (2007). Recent glacier retreat in the Caucasus Mountains, Russia, and associated increase in supraglacial debris cover and supra-/proglacial lake development. *Annals of Glaciology*, 46, 195–203. <https://doi.org/10.3189/172756407782871468>
- Tadono, T., Ishida, H., Oda, F., Naito, S., Minakawa, K., & Iwamoto, H. (2014). Precise global DEM generation by ALOS PRISM. In *ISPRS annals of the photogrammetry, remote sensing and spatial information sciences*, II–4 (pp. 71–76). <https://doi.org/10.5194/isprsannals-II-4-71-2014>
- Watson, C. S., King, O., Miles, E. S., & Quincey, D. J. (2018). Optimising NDWI supraglacial pond classification on Himalayan debris-covered glaciers. *Remote Sensing of Environment*, 217, 414–425. <https://doi.org/10.1016/j.rse.2018.08.020>
- Watson, C. S., Quincey, D. J., Carrivick, J. L., & Smith, M. W. (2016). The dynamics of supraglacial ponds in the Everest region, central Himalaya. *Global and Planetary Change*, 142, 14–27. <https://doi.org/10.1016/j.gloplacha.2016.04.008>
- Watson, C. S., Quincey, D. J., Carrivick, J. L., & Smith, M. W. (2017). Ice cliff dynamics in the Everest region of the central Himalaya. *Geomorphology*, 278, 238–251. <https://doi.org/10.1016/j.geomorph.2016.11.017>
- Watson, C. S., Quincey, D. J., Smith, M. W., Carrivick, J. L., Rowan, A. V., & James, M. R. (2017). Quantifying ice cliff evolution with multi-temporal point clouds on the debris-covered Khumbu Glacier, Nepal. <https://doi.org/10.1017/jog.2017.47>

References From the Supporting Information

- van Woerkom, T., Steiner, J. F., Kraaijenbrink, P. D. A., Miles, E. S., & Immerzeel, W. W. (2019). Sediment supply from lateral moraines to a debris-covered glacier in the Himalaya. *Earth Surface Dynamics*, 7(2), 411–427. <https://doi.org/10.5194/esurf-7-411-2019>